inventions

MDPI

Article

A Modeling-Based Flammable Risk Treatment of Refrigerant Leakage from a Commercial R-290 Refrigeration Machine

Mingkan Zhang *, Vishaldeep Sharma and Praveen Cheekatamarla

Oak Ridge National Laboratory, Oak Ridge, TN 37830, USA; sharmav@ornl.gov (V.S.); cheekatamapk@ornl.gov (P.C.)

* Correspondence: zhangm1@ornl.gov; Tel.: +1-865-241-6386

Abstract: Because of serious concerns about global warming, manufacturers have started phasing out high global warming potential (GWP) refrigerants in commercial refrigeration equipment (e.g., R-134a). As a potential replacement, propane (R-290) is an environmentally friendly refrigerant for commercial refrigeration equipment because its GWP is only three. However, propane is flammable and is therefore classified as a Class A3 refrigerant per ASHRAE Standards, so safety is a very important consideration when propane-based equipment is designed and deployed in buildings. In the event of a refrigerant leak, flammability of the refrigerant depends on the refrigerant's local concentration, which is highly affected by the indoor air environment, including temperature and air flow. In this study, a ventilation system attached to a commercial R-290 refrigeration device was designed to eliminate the flammability risk. Moreover, a computational fluid dynamics (CFD) model was developed to investigate the refrigerant leak, thereby evaluating effects of the ventilation system. The CFD model can visualize the flammable zones owing to the leak.

Keywords: low GWP refrigerants; flammable refrigerant leaking; CFD modeling; risk assessment

Citation: Zhang, M.; Sharma, V.; Cheekatamarla, P. A Modeling-Based Flammable Risk Treatment of Refrigerant Leakage from a Commercial R-290 Refrigeration Machine. *Inventions* **2024**, *9*, 53. https://doi.org/10.3390/inventions9030053

Academic Editors: Umberto Lucia, Giulia Grisolia and Debora Fino

Received: 27 March 2024
Revised: 30 April 2024
Accepted: 30 April 2024
Published: 4 May 2024

1. Introduction

Participants of the Montreal Protocol reached an agreement at their 28th Meeting of the Parties in October 2016 [1] to phase down hydrofluorocarbon (HFC) refrigerants because the world is facing the risks of global warming. Many studies have been conducted to seek alternative, lower global warming potential (GWP) refrigerants to replace the conventional, high GWP ones. However, according to ISO Standard 817 [2] and ANSI/ASHRAE Standard 34 [3], almost all the currently used alternative low GWP refrigerants are either categorized as A2 (mildly flammable) or A3 (flammable). The flammability of a flammable refrigerant is determined by the concentration of the refrigerant in air. The refrigerant is capable of producing a flash of fire in the presence of an ignition source if the concentration is between its lower flammability limit (LFL) and upper flammability limit (UFL). Therefore, safety is a very important consideration when designing and deploying low-GWP-refrigerant-based refrigeration equipment.

Many studies have been dedicated to the safe utilization of flammable low GWP refrigerants when a leakage occurs. In the early part of the 21st century, Zhao et al. [4] conducted a theoretical investigation of flammability for low GWP refrigerants, including R-32, R-143a, R-290, and R-600a. Their study focused on the effects of leak locations and operating conditions on flammable mixtures in refrigeration and air conditioning systems. Clodic and Riachi [5] developed a method to experimentally determine the flammability risk of different R-32 blends. Minor et al. [6], on the other hand, assessed the flammability characteristics of R-1234yf in a vehicle refrigeration system; they concluded that the potential for a flammable environment in the passenger compartment was low because, in most cases in their studies, the peak concentrations of R-1234yf were below its LFL. Nagaosa et al. [7] conducted a risk assessment for leakages of flammable refrigerants

into a closed space. They tested R-1234yf, R-32, R-152a, R-290, and R717 in their study, which showed that the risk of ignitions and flammability is different depending on the flammability characteristics of each refrigerant. Okamoto et al. [8] comprehensively studied the leakage of mildly flammable refrigerants (R-32, R-1234yf, R-290, and R-1234ze) into a room from a room air conditioner and a package air conditioner. A round-pipe microcrack leak model with crack opening displacement from 10 to 50 μm was built by Zhang et al. [9] to represent a true morphology of leak points of flammable refrigerant leakage, including R-290, R-32, and R-1234yf; their results revealed the influences of the crack size on the flammability of the leaking refrigerants. Elatar et al. [10] and Jung et al. [11] studied R-32 leaking from a rooftop unit and an outdoor unit, respectively, and evaluated the flammability risks of the R-32-based units. Although there are many studies dedicated to the leaking of flammable refrigerants, the visualization of flammable zones was rarely reported.

Among all of the low GWP refrigerants, propane (R-290) is one of the best alternatives to replace HFCs, not only because of its low GWP value (GWP = 3) [12], but also because of its high thermal performance and favorable thermodynamic properties for air conditioners and heat pumps. Therefore, significant attention has been recently focused on the study of R-290 leakage and its flammability in the community. Zhang et al. [13] and Zhang et al. [14] conducted experimental studies on the flammability hazards of an air conditioner using refrigerant R-290, including both indoor and outdoor units of a split air conditioner. In addition, a new quasi-liquid nitrogen method was developed to investigate the refrigerant distribution in R-290 split-type household air conditioners and the leaking rate under various conditions [15]. Ning et al. [16] investigated the leakage hazard control of an R290 split-type household air conditioner with 5 mm diameter finned-tube heat exchangers under off-mode through concentration measurement and ignition experiment. Recently, Li et al. [17] developed a numerical model of refrigerant leakage to assess the explosion risk analysis of R-290 leakage into a limited external space. Although R-290 is becoming a popular choice for commercial refrigeration device such as vending machines and ice cream machines, there are not many studies focusing on commercial refrigeration devices.

Two main methods were employed to study the flammability risk of leaking flammable refrigerants, the experimental approaches, and the numerical modeling studies. Among the methods, computational fluid dynamics (CFD) was the dominant tool [6–11,18] used by most of the numerical studies on the flammability risk of leaking flammable refrigerants. CFD simulations can provide a reliable prediction of fluid flow and concentration distribution of refrigerants in the simulation domain with an economic cost comparable to experimental studies. In the present work, a 3D CFD model was developed to assess the flammability risk of R-290 leaking from a commercial refrigeration system. Using postprocessing tools, one can also directly visualize the zones with flammable risk by plotting the zones that have refrigerant concentration between the LFL and UFL. Moreover, evolution of the flammable zones can also be monitored by plotting them in different time frames. A ventilation system was designed to attach to the commercial refrigeration system to eliminate the flammability risk of the leaking R-290. Effects of the ventilation system have been evaluated using simulation results from the CFD model.

2. Materials and Methods

A 3D CFD model was developed to evaluate the design for eliminating the flammable risk of R-290 leaking from a commercial refrigeration system. A commercial software, ANSYS/FLUENT [19] (version 17.2), was employed to build the model and conduct the simulations. The model was composed of a commercial refrigeration device with attached ventilation and a small room where the refrigeration system was located.

Figure 1 depicts the schematic view of the CFD model in the present work in a room measuring L = 3.0 m, H = 4.0 m, and W = 2.0 m. A ventilation system was attached to the commercial refrigeration machine, which connects to the top of the room. In the refrigeration device model, some cylinders represented the components in the machine as blockages that affect the air flow and refrigerant distribution. The room and the refrigeration

machine were assumed to both be geometrically symmetric, so only half of them were built in the model.

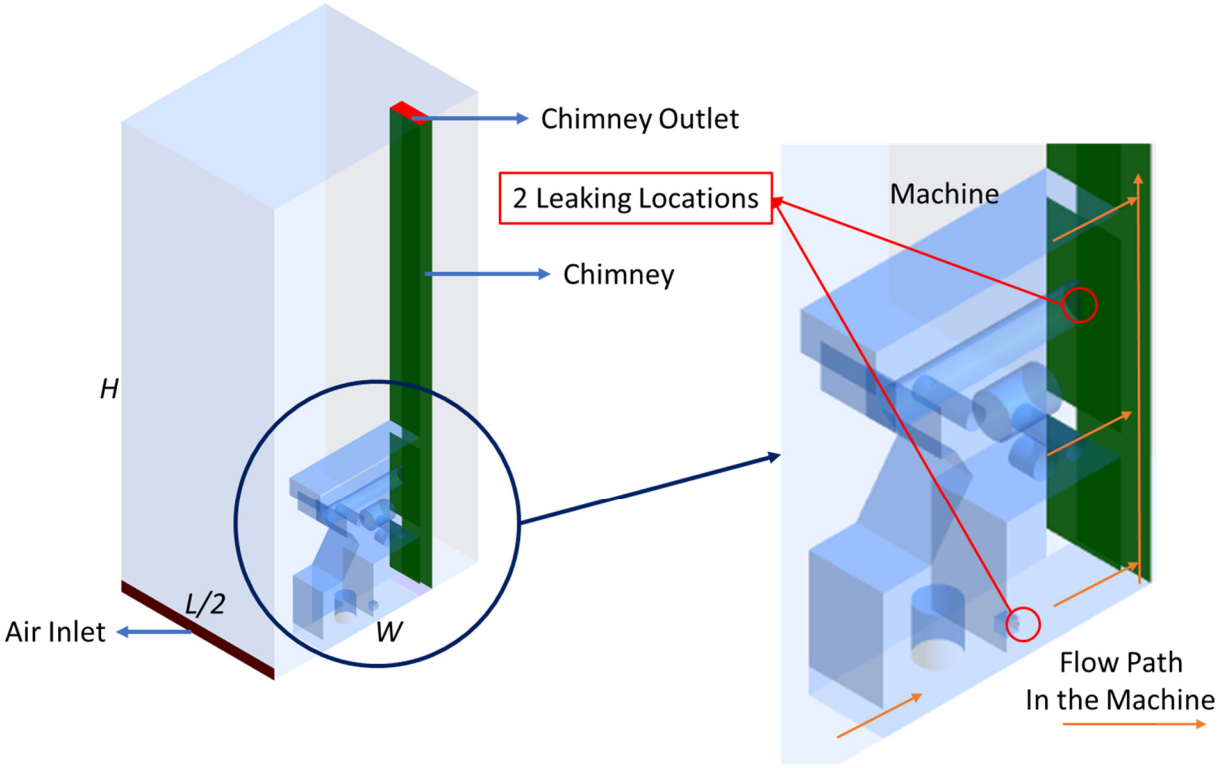

Figure 1. A schematic view of the CFD model.

The governing equations of the CFD model include a continuity equation for mass conservation, a momentum equation for gas flow, and energy equations for heat transfer. Here, two gases—air and R-290—were modeled. To describe the distribution of R-290 in the air, a mixture model was employed. The continuity equation is as follows:

$$\frac{\partial \rho}{\partial t} + \frac{\partial (\rho u_i)}{\partial x_i} = 0, \tag{1}$$

where u and ρ are the mass averaged velocity and the mixture density, respectively, which are given by Equations (2) and (3):

$$u = \frac{\alpha_l \rho_l u_l}{\rho}, \tag{2}$$

and

$$\rho = \alpha_l \rho_l. \tag{3}$$

In Equations (2) and (3), α_l is the volume fraction of gas l. The subscripts $l = 1$ and $l = 2$ represent air and R-290, respectively. Notably, the variables without subscript l are the ones for the entire mixture.

Next, the momentum equation can be written as follows:

$$\frac{\partial (\rho u_i)}{\partial t} + \frac{\partial (\rho u_i u_j)}{\partial x_j} = -\frac{\partial p}{\partial x_i} + \frac{\partial}{\partial x_j}\left[\mu\left(\frac{\partial u_j}{\partial x_i} + \frac{\partial u_i}{\partial x_j} - \frac{2}{3}\delta_{ij}\frac{\partial u_k}{\partial x_k}\right) - \rho\overline{u_i' u_j'}\right] + F + \nabla \cdot (\alpha_l \rho_l (u_{j,l} - u_j)(u_{j,l} - u_j)), \tag{4}$$

where p and μ are pressure and dynamic viscosity, respectively; and F is the gravitational body force, which is described by a Boussinesq approximation. The equation for μ is as follows:

$$\mu = \alpha_l \mu_l. \tag{5}$$

The incompressible ideal gas model was implemented for both air and R-290 because of the room temperature and pressure conditions in the present work. A k-ε model was adopted to simulate turbulent flow in the model, so the Reynolds Stress term is as follows:

$$-\rho\overline{u_i' u_j'} = \mu_t\left(\frac{\partial u_j}{\partial x_i} + \frac{\partial u_i}{\partial x_j}\right) - \frac{2}{3}\left(\rho k + \mu_t \frac{\partial u_k}{\partial x_k}\right)\delta_{ij}, \tag{6}$$

where μ_t is the turbulence dynamic viscosity. It can be calculated by introducing turbulence kinetic energy k and turbulence dissipation rate ε as follows:

$$\mu_t = \rho C_\mu \frac{k^2}{\varepsilon}, \tag{7}$$

$$\frac{\partial(\rho k)}{\partial t} + \frac{\partial(\rho k u_i)}{\partial x_i} = \frac{\partial}{\partial x_j}\left[\left(\mu + \frac{\mu_t}{\sigma_k}\right)\frac{\partial k}{\partial x_j}\right] - \rho\overline{u_i' u_j'}\frac{\partial u_j}{\partial x_i} - \rho\varepsilon, \tag{8}$$

$$\frac{\partial(\rho\varepsilon)}{\partial t} + \frac{\partial(\rho\varepsilon u_i)}{\partial x_i} = \frac{\partial}{\partial x_j}\left[\left(\mu + \frac{\mu_t}{\sigma_\varepsilon}\right)\frac{\partial \varepsilon}{\partial x_j}\right] - C_{1\varepsilon}\frac{\varepsilon}{k}\left(\rho\overline{u_i' u_j'}\frac{\partial u_j}{\partial x_i}\right) - C_{2\varepsilon}\rho\frac{\varepsilon^2}{k}. \tag{9}$$

In the previous equations, the parameters C_μ = 0.09, $C_{\varepsilon 1}$ = 1.44, $C_{\varepsilon 2}$ = 1.92, σ_k = 1, and σ_ε = 1.3 are from [19].

The energy equation in the mixture model form is as follows:

$$\frac{\partial}{\partial t}\alpha_l \rho_l h_l + \frac{\partial}{\partial x_j}[\alpha_l u_{j,l}(\rho_l h_l + p)] = \nabla\cdot(\lambda_{\text{eff}}\nabla T) \tag{10}$$

where λ_{eff} is the effective conductivity, and h_l is the enthalpy for gas l.

To validate the CFD model, the experimental data for a leak from an indoor room air conditioner (RAC) unit into a single room were employed to compare with the CFD simulation results under the same conditions. The experiment was reported by Okamoto et al. [8], in which a wall-mounted indoor RAC was located on one of the walls of a room. The refrigerant in the RAC is R-32 in their experiments, which leaked from the RAC to the room with a leaking rate of 250 g/min. The total charge was 1 kg, so it took 4 min for all R-32 to leak from the RAC to the room. The leaking was from an indoor unit air outlet with dimensions of 0.6 m × 0.06 m in the experiment. The dimensions of the indoor unit were 0.6 m × 0.24 m × 0.3 m. To monitor the R-32 concentration distribution, six data points were deployed vertically in the testing room, starting with point 1 at the floor level. Then, the history of concentration of R-32 of the six points was recorded after the leaking started. The experiment was reproduced using our CFD model in which the same conditions (e.g., room size, RAC size, leaking rate, and properties of R-32) were employed as in their experiment. Then, from the CFD simulations, curves were plotted to reveal the concentration history of R-32 at the same points as those used in the experiment.

Figure 2 shows the comparison—and great agreement—between the experimental data and CFD results. All data from the CFD modeling were within the error bar of the experimental results, as shown in Figure 2, although the comparisons present some overprediction of the R-32 concentration at lower sampling points (i.e., points 1–4) from the CFD model. Therefore, the CFD model can successfully simulate and capture the refrigerant leak dispersion inside the room with acceptable accuracy. Because refrigerant leak dispersion inside the room depends mainly on the refrigerant density, the validated CFD model can be used to study not only R-32 leaking but also leaking of other refrigerants, such as R-290.

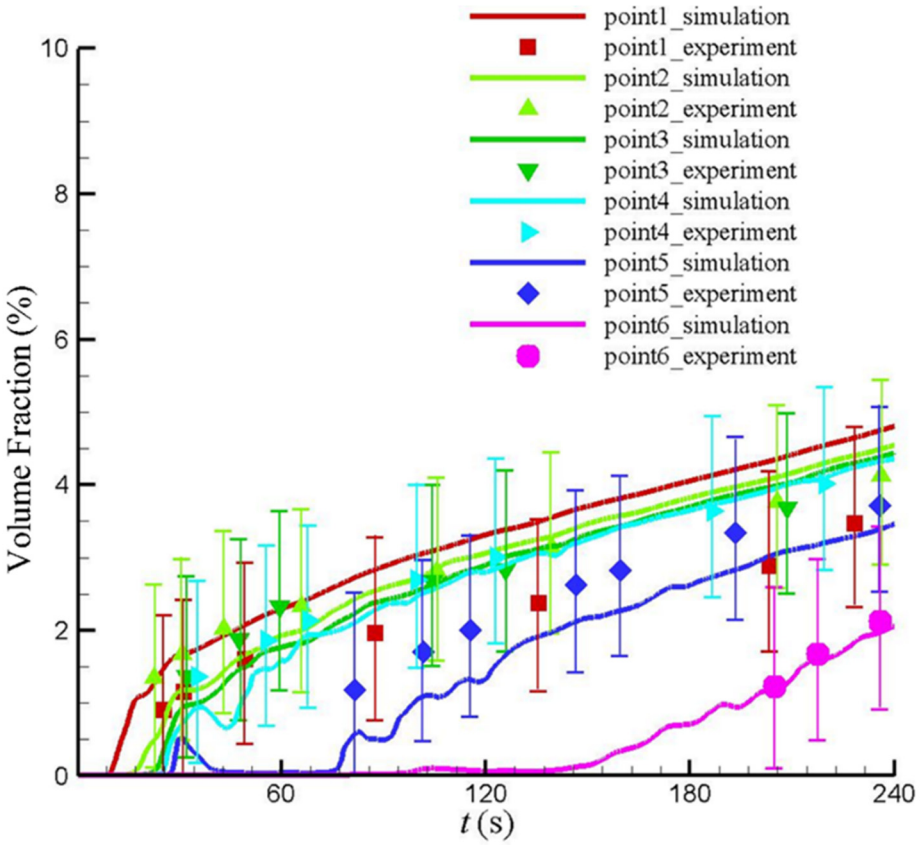

Figure 2. Validation by comparing CFD results (lines) with experimental data (symbols) from Okamoto et al. [8].

3. Results and Discussion

In this paper, propane leaking from a commercial refrigeration device was investigated; two leaking points were modeled. The first leaking point was located in a small chamber at the lower part of the refrigeration device, which is called the lower leaking point in this paper. This small chamber is semi-insulated from the other part of the device. The only connection between the chamber and the rest of the device is a small window. The second leaking point is out of the chamber, close to the top of the device, and is called the higher leaking point. The modeled leaking points represent two typical locations of leaking in the device, and they are depicted in Figure 1. Our experimental testing indicated that the temperature deviation was trivial when the leaking happened, so to simplify the model in the present work, it is assumed that the leaking of R-290 occurs at room temperature at the leaking locations of the refrigeration device. Two leaking rates, 150 g/min and 300 g/min, were tested using the CFD model. In all simulations, the leaking duration was 1 min, so the total leaked R-290 is 150 g and 300 g in the low and high leaking rate cases, respectively. To evaluate the effectiveness of the current design for eliminating R-290 flammability risk, the cases when ventilation is off were simulated as the baseline cases, in which the flammability risk of leaking R-290 was demonstrated without the current design. On the other hand, cases with a fixed ventilation rate (50 CFM) were also simulated to compare with the baseline cases.

Figure 3a shows that the average volume fraction of R-290 in the refrigeration device changes with time when the leaking location is in a lower position. As expected, the higher R-290 leaking rate leads to a higher peak volume fraction in the device before the leaking stops (t = 1 min). Interestingly, the peak volume fraction in the device when the ventilation is on is higher than that of the baseline case with the same leaking rate. This occurs because, when the ventilation is off, the leaked R-290 escapes from the chamber to the device and then to the room. Because the density of R-290 is much higher than the density of air, the

R-290 in the room accumulates near the ground. Figure 4 depicts the contours of the R-290 volume fraction without ventilation when the leaking rates are 150 g/min and 300 g/min, which reveals R-290 can escape from the device to the room after 1 min of leaking without ventilation. On the other hand, Figure 5 shows the contours of the R-290 volume fraction when the ventilation is on. Because of the low pressure created by the ventilation fan, the high-density R-290 runs upward in the device instead of escaping to the room. As a result, if the leaking occurs at the lower leaking point, when the ventilation is on, the peak volume fraction of the device is always higher than that of the baseline cases with the same leaking rate. However, considerable R-290 remains in the device after 10 min from the start of leaking (i.e., the average volume fractions are about 7% and 4% for high and low leaking cases, respectively). The history of the R-290 distributions can also be observed from Figures 4 and 5 for ventilation off and on scenarios, respectively. In the baseline cases, as shown in Figure 4, after the leaking stops, R-290 starts to escape from the chamber to the device and then to the room, owing to the density difference. Because the ventilation is off, the R-290 escapes at a slow speed. Although some R-290 escapes to the room, most of the R-290 still accumulates in the device after 10 min. Figure 3a also reveals that, when the ventilation is working, all the R-290 is exhausted from the device for both low and high leaking rates after 10 min. Figure 5 shows the history of the distribution of volume fraction of R-290 changing with time when the ventilation is on; when the leaking stops (t = 1 min), no R-290 escapes to the room, as described previously. When t = 5 min, all the R-290 is exhausted from the device except for what is in the chamber. The ventilation continues working, so that when t = 10 min, no R-290 remains anywhere in the device, including in the chamber. It is very interesting that, when t = 5 min, the average R-290 volume fraction in the device from the high leaking rate case is lower than that of the low leaking rate case (see Figures 3 and 5), leading to less R-290 remaining in the device when the leaking rate is high. A higher leaking rate results in a higher exhausting rate (the higher slope of the black curve in Figure 3 from t = 2 min to t = 3 min). This occurs because the density of R-290 is much higher than the density of air, which makes R-290 sink to the bottom of the device. On the other hand, ventilation exhausts the air/R-290 mixture from the top of the device, leading to an upward flow. The higher leaking rate creates a more significant convection flow, sending more R-290 to the ventilation to be exhausted. Therefore, a higher leaking rate provides a higher exhausting rate.

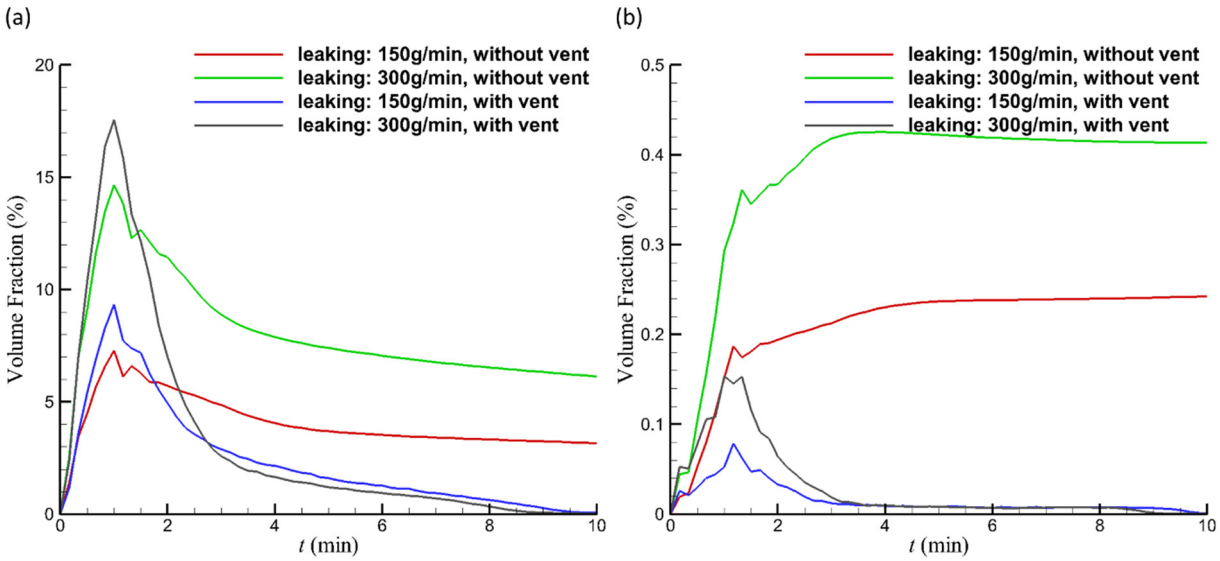

Figure 3. Average volume fraction of R-290 in the refrigeration device (**a**) and in the rest of the room (**b**) changes with time when the leaking location is low.

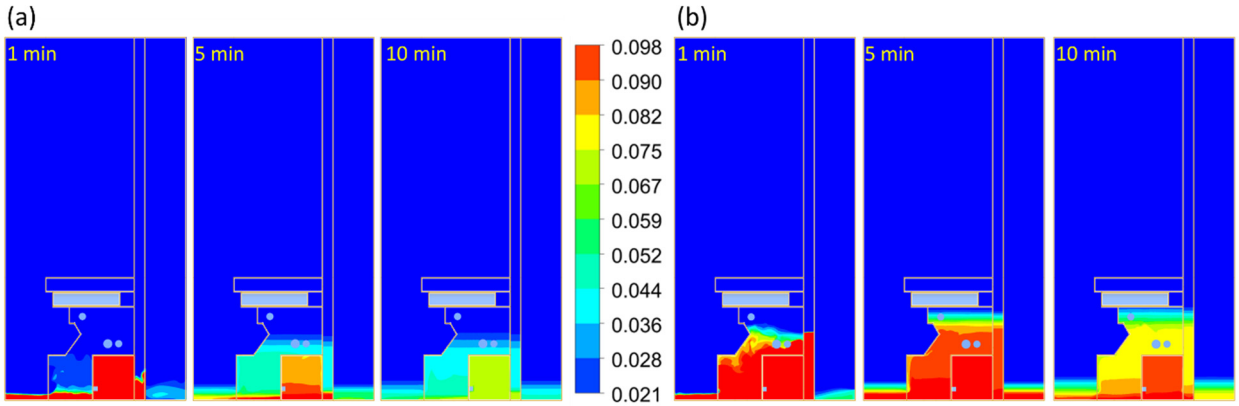

Figure 4. Distribution of the volume fraction of R-290 in the plane of symmetry changes with time when the ventilation is off, the leaking location is low, and the leaking rates are (**a**) 150 g/min and (**b**) 300 g/min.

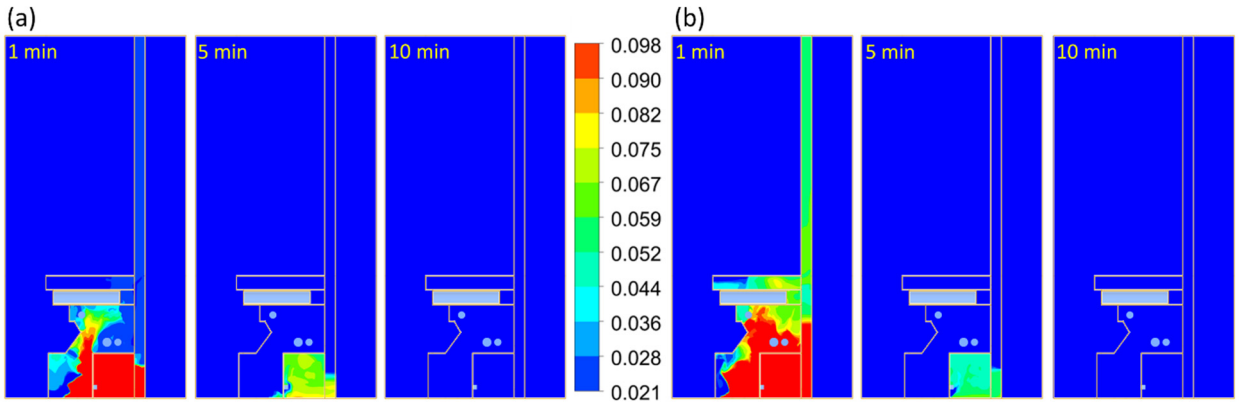

Figure 5. Distribution of the volume fraction of R-290 in the plane of symmetry changes with time when the ventilation is on, the leaking location is low, and the leaking rates are (**a**) 150 g/min and (**b**) 300 g/min.

Figure 3b shows the average volume fraction of escaping R-290 to the room for both leaking rates and ventilation on/off. Notably, the room has a relatively huge volume, but R-290 sinks to the bottom of the room; therefore, the average volume fraction can only index the quality of escaping R-290 to the room but cannot reveal the flammability of R-290 in the room. When the ventilation is on, R-290 reaches a peak before the leaking stops. After 10 min, all the R-290 is exhausted from the room owing to the ventilation.

To directly visualize the flammability of R-290 leaking, the flammable zones are depicted in Figures 6 and 7 for both flow rates and ventilation on/off when the leaking location is low. A flammable zone is the space in which the volume fraction of R-290 is between its LFL (2.05%) and UFL (9.8%) [20]; in the flammable zone, the R-290 is capable of producing a flash of fire in the presence of an ignition source. The flammable zones are marked in red in Figures 6 and 7, whereas the zones without color in Figures 6 and 7 can be regarded as safety zones.

Figure 6 shows that in the case without ventilation, when the leaking stops (t = 1 min), the chamber is not flammable because the R-290 volume fraction is higher than its UFL for both leaking rates. A part of the device is flammable when t = 1 min, in which the high leaking rate leads to a larger flammable zone in the device. For both leaking rates, the thin layer of the room near the ground is flammable. When t = 10 min, the chambers of both leaking rates are flammable, whereas in the low and high leaking cases, about a half and two-thirds of the device are flammable, respectively. In the room, when t = 10 min, the heights of the flammable zone are 0.20 and 0.26 m in the low and high leaking cases, respectively.

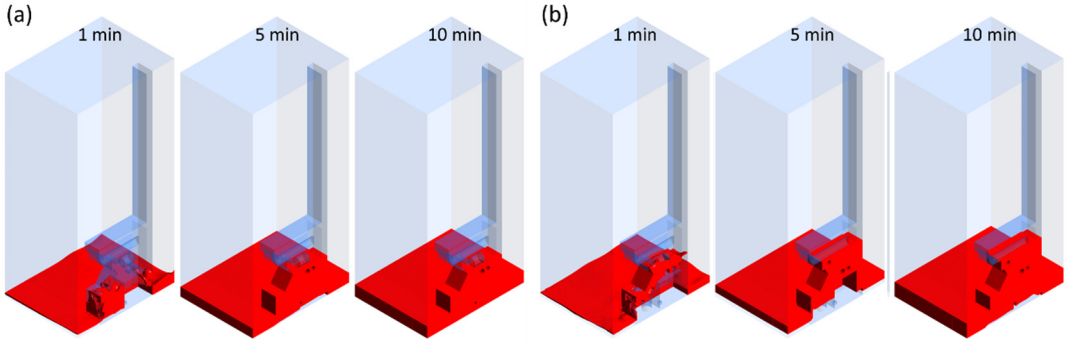

Figure 6. Flammable zone changes with time when the ventilation is off, the leaking location is low, and the leaking rates are (**a**) 150 g/min and (**b**) 300 g/min.

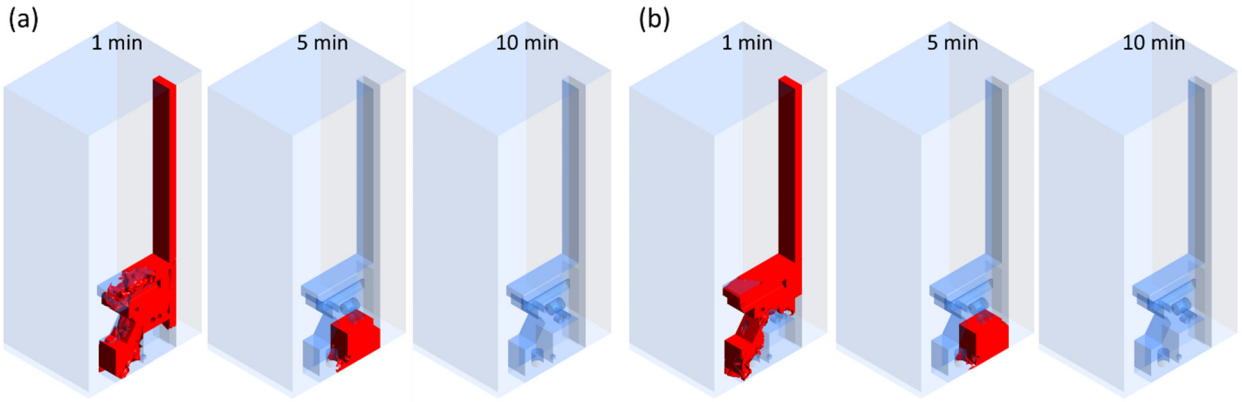

Figure 7. Flammable zone changes with time when the ventilation is on, the leaking location is low, and the leaking rates are (**a**) 150 g/min and (**b**) 300 g/min.

Figure 7 shows how the ventilation works to eliminate the flammable risk when leaking happens at the low leaking location. Comparing Figure 7a,b, for both leaking rates, the flammable zones are very similar at the same time, although the volume fraction distributions are different (see Figure 5). The only difference occurs when t = 1 min, at which time the flammable zone of the high leaking case is slightly larger than that of the low leaking rate case because more R-290 is leaked in the device. Therefore, the following discussion will not differ for the two leaking rate cases. Figure 7 shows that, after leaking stops, when the ventilation is on, almost the entire device except the chamber and the chimney are flammable. The chamber is not flammable because the R-290 volume fraction is higher than its UFL. When t = 10 min, all the R-290 has been exhausted, as shown in Figure 7.

When the leaking location is high, the leaking point is out of the chamber, so the spreading of R-290 is much easier than that of the low leaking location cases. Figure 8a shows that the average volume fraction in the refrigeration device changes with time when the leaking location is high. Comparing Figure 3a with Figure 8a, the peak of the average volume fractions of the high leaking location is much higher than the low leaking location in the baseline cases (green and red curves at t = 1 min). Because the density of R-290 is higher than the density of air, without ventilation, the R-290 sinks from the top of the device to the bottom after leaking, thus delaying the escape of the R-290 to the room. As a result, the peaks of the green and red curves in Figure 8a are higher than the curves with the same colors in Figure 3a. Figure 9 depicts the distributions of R-290 before the leaking stops. It shows R-290 spreads to the entire device, including half of the chamber, for both leaking rates. After leaking stops, R-290 escapes from the device to the room as shown in Figure 9, so the green and red curves drop in Figure 8a. On the other hand, because the leaking occurs out of the chamber, exhausting it is easier when the ventilation is on. As shown in Figure 8a, the peaks of the black and blue curves (about 5.5% and 3%) are

much lower than the ones (about 17.5% and 9.5%) in Figure 3a, respectively, indicating a quick exhaustion due to the ventilation. According to Figure 8a, when t = 3 min, all R-290 has been exhausted from the device for both leaking rates. Figure 8b shows the average volume fraction in the rest of the room changes with time when the leaking location is high. Figure 8b indicates that, without ventilation, when the leaking location is high, the spreading of R-290 to the room is slower than that of the low leaking location cases as described previously. However, when t = 10 min, the green and red curves in Figure 8a are almost as high as the same curves in Figure 3a. Therefore, it can be concluded that, when t = 10 min, the R-290 that escapes into the room does not depend on the leaking location without ventilation. If the ventilation is on, very little R-290 can escape during the leaking. Then, it is quickly exhausted, according to Figures 8b and 10.

Figure 11 depicts the flammable zones at different times when the ventilation is off and the leaking location is high. When t = 1, about half the device is flammable in the low leaking rate case, whereas the other half is not flammable because the R-290 volume fraction is higher than its UFL. At the same time, Figure 11b shows that only a small part of the device is flammable in the high leaking rate case because the R-290 volume fraction is higher than its UFL in most of the device. When t = 10 min, for both leaking rates, the entire device and the bottom of the room are flammable.

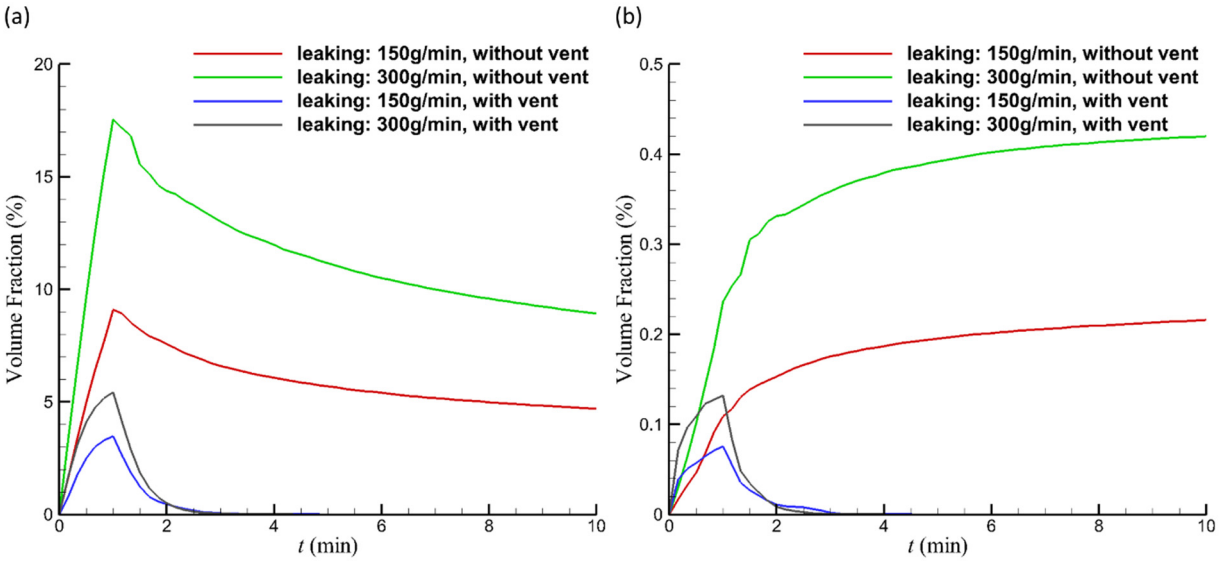

Figure 8. Average volume fraction in (**a**) the refrigeration device and (**b**) the rest of the room changes with time when the leaking location is high.

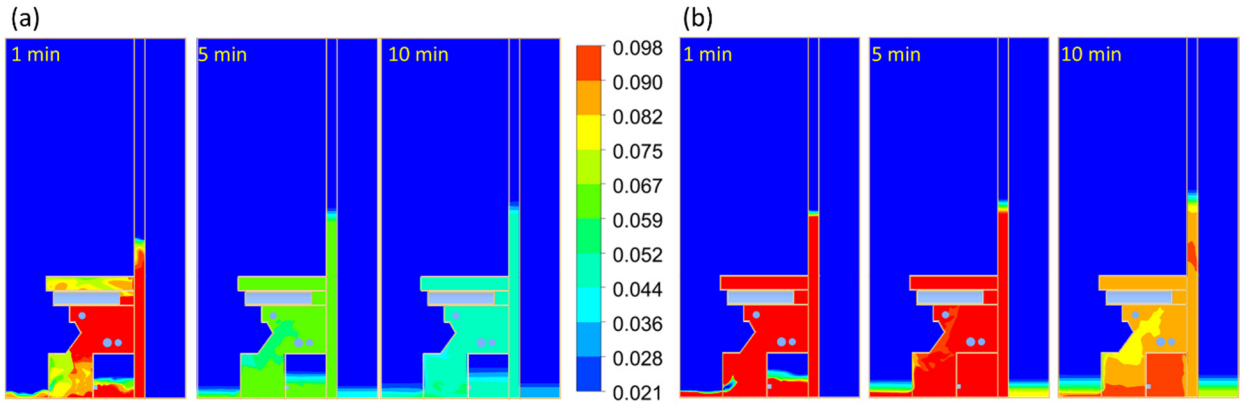

Figure 9. The distribution of volume fraction of R-290 in the plane of symmetry changes with time when the ventilation is off, the leaking location is high, and the leaking rates are (**a**) 150 g/min and (**b**) 300 g/min.

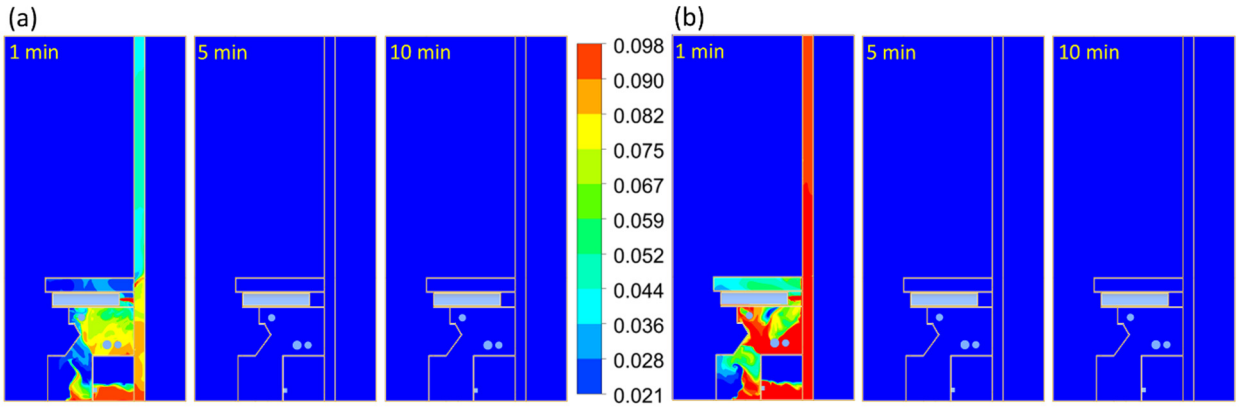

Figure 10. The distribution of volume fraction of R-290 in the plane of symmetry changes with time when the ventilation is on, the leaking location is high, and the leaking rates are (**a**) 150 g/min and (**b**) 300 g/min.

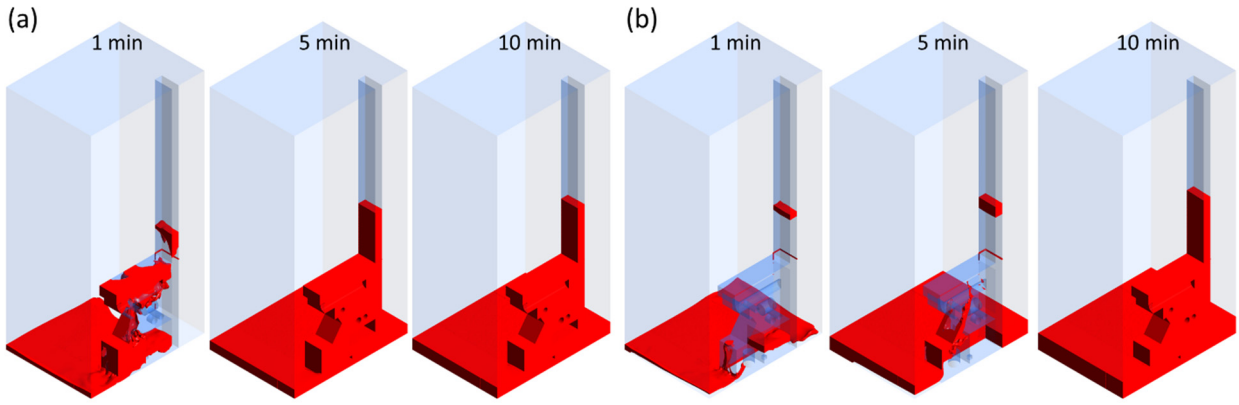

Figure 11. Flammable zone changes with time when the ventilation is off, the leaking location is high, and the leaking rates are (**a**) 150 g/min and (**b**) 300 g/min.

If the ventilation is on (Figure 12), when 10 min have passed, for both leaking rates, there does not exist a flammable zone anywhere in the simulation domain because all the R-290 has been exhausted within 2 min after the leaking stops (t = 3 min). When t = 1 min, the flammable zone in the device from the low leaking rate case is larger than that of the high leaking rate case because the high leaking rate case has a larger zone in which the R-290 volume fraction is higher than the UFL.

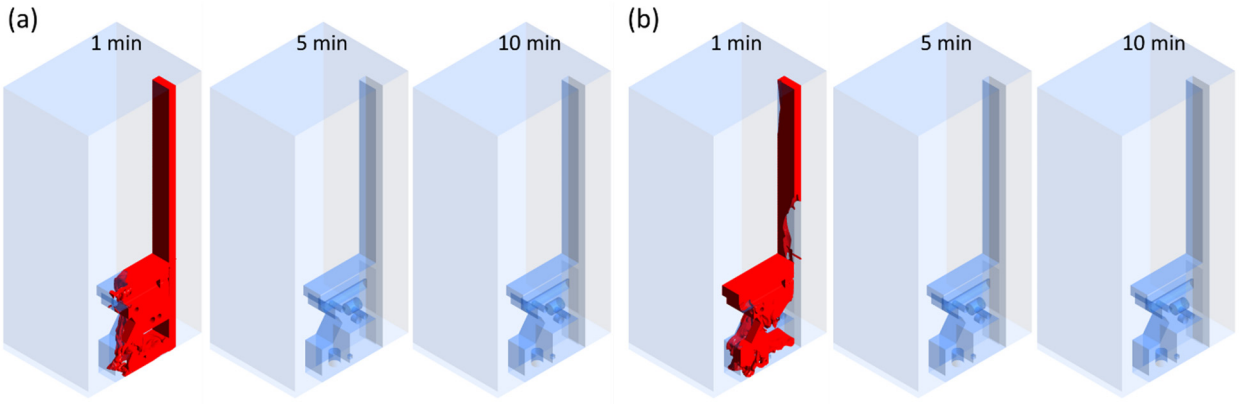

Figure 12. Flammable zone changes with time when the ventilation is on, the leaking location is high, and the leaking rates are (**a**) 150 g/min and (**b**) 300 g/min.

Although the model can successfully track the R-290 concentration and visualize the flammable zone of R-290, this study still has some limitations. In the CFD model, it is assumed that the leaking is from holes D = 1 mm. However, in real leaking scenarios, R-290 could leak from a small hole or a crack. The size and shape of the leaking source could influence the distribution of R-290, which is not included in the present model. On the other hand, the model lacks control of the ventilation system. In real applications, the ventilation fan needs to be controlled by a control strategy with a censor, i.e., when the sensor detects concentration of R-290 is higher than 100 ppm, the ventilation will be turned on. The control strategy will be included in future research.

4. Conclusions

A ventilation system attached to a commercial R-290 refrigeration device was designed to eliminate the flammability risk both inside and outside of the device when leaking of a flammable refrigerant occurs. A CFD model was developed to evaluate the effects of the ventilation system by simulating the R-290 leaking process, tracking the concentration of the refrigerant, and plotting the flammable zones inside and outside of the device for the cases with ventilation on and off. Two leaking rates and two leaking locations were also tested to evaluate the ventilation system in different scenarios.

The simulation results show that all the simulations reach a steady state after 10 min in the present work. The results indicate that the ventilation system can effectively exhaust the flammable R-290 from both device and room space in a short time (10 min for the low leaking location and 3 min for the high leaking location) to reduce the flammable risk from the leaking. In comparison, without the ventilation system, when the leaking location is low, part of the refrigeration device is flammable after 10 min, whereas the entire device is flammable after 10 min when the leaking location is high. It was also found that, without ventilation, a thin layer of the room near the ground is flammable owing to the higher density of R-290. The thickness of the layer depends on the R-290 leaking rate.

Some interesting phenomena were also observed from the simulation results:

1. When the leaking location is high and the leaking rate is low, without ventilation during the initial 5 min, the chamber where the leaking point is located is almost non-flammable because the volume fraction of R-290 is too high to be above the UFL in the chamber.
2. When the leaking location is high and the leaking rate is also high, without ventilation during the initial 5 min, the device is almost non-flammable because the volume fraction of R-290 is also above the UFL in most parts of the device in this case.
3. When the leaking location is low and ventilation is on, after t = 3 min, the R-290 concentration of the device in the high leaking rate case is even lower than that of the low leaking rate case. This can be attributed to the high convection in the high leaking rate case leading to a high exhausting speed.
4. Based on the simulation results, it is recommended to install the ventilation system attached to the commercial refrigeration device due to the flammability of R-290. It is also recommended to install a duct directly to the insulated chamber in the device to avoid the accumulation of R-290 in the chamber. Future research will be focusing on improving the current ventilation design, e.g., adding a control strategy to the fan based on values from the gas sensor.

Author Contributions: Conceptualization, V.S. and P.C.; Methodology, M.Z.; Validation, M.Z.; Investigation, M.Z., V.S. and P.C.; Writing—original draft, M.Z.; Writing—review & editing, V.S. and P.C.; Project administration, V.S. and P.C. All authors have read and agreed to the published version of the manuscript.

Funding: This manuscript has been authored by UT-Battelle, LLC, under contract DE-AC05-00OR22725 with the US Department of Energy (DOE). The US government retains and the publisher, by accepting the article for publication, acknowledges that the US government retains a nonexclusive, paid-up, irrevocable, worldwide license to publish or reproduce the published form of this manuscript, or

allow others to do so, for US government purposes. DOE will provide public access to these results of federally sponsored research in accordance with the DOE Public Access Plan (http://energy.gov/downloads/doe-public-access-plan) (accessed on 1 April 2024).

Data Availability Statement: The data that support the findings of this study are available from the corresponding author, M.Z., upon reasonable request.

Acknowledgments: This work was sponsored by the U.S. Department of Energy's Building Technologies Office. The authors would like to acknowledge Payam Delgoshaei, the Department of Energy (DOE) Building Technologies Office (BTO), for their support.

Conflicts of Interest: The authors declare no conflicts of interest.

References

1. United Nations. Report of the Twenty—Eighth Meeting of the Parties to the Montreal Protocol on Substances That Deplete the Ozone Layer. In Proceedings of the Twenty-Eighth Meeting of the Parties to the Montreal Protocol, Kigali, Rwanda, 10–15 October 2016; p. 72.
2. *ISO 817:2014*; Refrigerants—Designation and Safety Classification. ISO: Geneva, Switzerland, 2014. Available online: https://www.iso.org/standard/52433.html (accessed on 15 January 2023).
3. *ASHRAE 34-2019*; Designation and Safety Classification of Refrigerants. ASHRAE: Atlanta, GA, USA, 2019; pp. 1–4.
4. Zhao, Y.; Yie, L.; Zhengguo, Z. Investigation of Flammability for Alternative Mixtures in Air Conditioner and Refrigeration Systems. *J. Fire Sci.* **2001**, *19*, 242–251. [CrossRef]
5. Clodic, D.; Riachi, Y. A Method for Determining Practical Flammability Risk When Using Refrigerant Blends. *HVACR Res.* **2009**, *15*, 819–834. [CrossRef]
6. Minor, B.H.; Herrmann, D.; Gravell, R. Flammability Characteristics of HFO-1234yf. *Process Saf. Prog.* **2010**, *29*, 150–154. [CrossRef]
7. Nagaosa, R.; Aute, V.C.; Radermacher, R. A Risk Assessment for Leakages of Flammable Refrigerants into a Closed Space. *Int. Refrig. Air Cond. Conf.* **2012**, *2240*, 1–10.
8. Okamoto, H.; Hattori, T.; Dang, C.; Hihara, E. Leakage of Mildly Flammable Refrigerants into a Room. *Int. Refrig. Air Cond. Conf.* **2014**. Available online: https://docs.lib.purdue.edu/iracc/1496/ (accessed on 1 April 2024).
9. Zhang, S.; Chen, G.; Li, Z.; Fang, J. Computational Fluid Dynamics Analysis of Flammable Refrigerant Leakage through a Microcrack. *Int. J. Refrig.* **2022**, *134*, 35–44. [CrossRef]
10. Elatar, A.; Abu-Heiba, A.; Patel, V.; Edwards, K.D.; Baxter, V.; Abdelaziz, O.; Zhang, M. Evaluation of Flammable Volume in the Case of a Catastrophic Leak of R-32 from a Rooftop Unit. *Int. J. Refrig.* **2018**, *91*, 39–45. [CrossRef]
11. Jung, G.; Han, U.; Lee, H. Numerical Investigation on Flammability of R32 Leakage in Heat Pump Outdoor Unit with CFD Simulation. *Int. J. Air-Cond. Refrig.* **2023**, *31*, 19. [CrossRef]
12. Hodnebrog, Ø.; Dalsøren, S.B.; Myhre, G. Lifetimes, Direct and Indirect Radiative Forcing, and Global Warming Potentials of Ethane (C2H6), Propane (C3H8), and Butane (C4H10). *Atmos. Sci. Lett.* **2018**, *19*, e804. [CrossRef]
13. Zhang, W.; Yang, Z.; Zhang, X.; Lv, D.; Jiang, N. Experimental Research on the Explosion Characteristics in the Indoor and Outdoor Units of a Split Air Conditioner Using the R290 Refrigerant. *Int. J. Refrig.* **2016**, *67*, 408–417. [CrossRef]
14. Zhang, Y.; Liu, C.; Wang, T.; Pan, L.; Li, W.; Shi, J.; Chen, J. Leakage Analysis and Concentration Distribution of Flammable Refrigerant R290 in the Automobile Air Conditioner System. *Int. J. Refrig.* **2020**, *110*, 286–294. [CrossRef]
15. Tang, W.; He, G.; Cai, D.; Zhu, Y.; Zhang, A.; Tian, Q. The Experimental Investigation of Refrigerant Distribution and Leaking Characteristics of R290 in Split Type Household Air Conditioner. *Appl. Therm. Eng.* **2017**, *115*, 72–80. [CrossRef]
16. Ning, Q.; He, G.; Fan, M.; Xiong, J.; Li, X. Flammable Refrigerant Leakage Hazards Control for Split-Type Household Air Conditioners. *Int. J. Refrig.* **2022**, *144*, 188–201. [CrossRef]
17. Li, Y.; Yang, J.; Wu, X.; Zhou, P.; Liu, Y.; Han, X. Explosion Risk Analysis of R290 Leakage into a Limited External Space. *Appl. Therm. Eng.* **2023**, *225*, 120122. [CrossRef]
18. Liu, Q.; Zhang, H.; Liu, Y.; Huang, H.; Zhang, X.; Li, Z.; Yao, W. Influencing Factors of Flammable Refrigerants Leaking in Building Airconditioning System. *Procedia Eng.* **2013**, *62*, 648–654. [CrossRef]
19. *ANSYS FLUENT 17.2 Theory Guide*; ANSYS: Canonsburg, PA, USA, 2017.
20. Cashdollar, K.L.; Zlochower, I.A.; Green, G.M.; Thomas, R.A.; Hertzberg, M. Flammability of Methane, Propane, and Hydrogen Gases. *J. Loss Prev. Process Ind.* **2000**, *13*, 327–340. [CrossRef]